11098 *Inorg. Chem.* **2009**, *48*, 11098–11107
DOI: 10.1021/ic901488j

Inorganic Chemistry
Article

DNA-Cleavage Induced by New Macrocyclic Schiff base Dinuclear Cu(I) Complexes Containing Pyridyl Pendant Arms

Arnau Arbuse,[†] Marc Font,[†] Ma Angeles Martínez,[*,†] Xavier Fontrodona,[‡] Ma José Prieto,[∥] Virtudes Moreno,[§] Xavier Sala,[⊥] and Antoni Llobet[*,⊥,#]

[†]*Departament de Química,* [‡]*Serveis Científico-Tècnics Universitat de Girona, Campus de Montilivi, E-17071 Girona, Spain,* [§]*Departament de Química Inorgànica,* [∥]*Departament de Microbiologia Universitat de Barcelona, Martí i Franquès 1-11, E-08028 Barcelona, Spain,* [⊥]*Institute of Chemical Research of Catalonia (ICIQ), Av. Països Catalans 16, E-43007 Tarragona, Spain, and* [#]*Departament de Química, Universitat Autònoma de Barcelona, Ceranyola del Vallès, E-0194 Barcelona, Spain*

Received July 27, 2009

A new series of dinuclear Cu(I) complexes with hexaazamacrocyclic Schiff base ligand containing pyridyl pendant arms has been synthesized and characterized. The solid-state structures of $[Cu_2^I(bsp3py)](CF_3SO_3)_2$ (**1**$(CF_3SO_3)_2$), $[Cu_2^I(bsm3py)](SbF_6)_2$ (**2**$(SbF_6)_2$), and $[Cu_2^I(bsp2py)](CF_3SO_3)_2$ (**3**$(CF_3SO_3)_2$) have been established by single-crystal X-ray diffraction analysis. The geometries of the copper centers in all three cases are almost identical showing a distorted tetrahedral coordination, very close to a trigonal pyramidal arrangement. Interactions of complexes with calf thymus DNA have been investigated by circular dichroism spectroscopy (CD) which suggests that the interaction for each complex is a nonintercalative mode with regard to DNA. The electrophoretic mobility study and the atomic force microscopy (AFM) in the presence of H_2O_2 reveal a cleavage of pBR322 supercoiled DNA that depends on the nature of the Cu(I) complex used. The most efficient reactivity is observed for complexes **1**$(CF_3SO_3)_2$ and **2**$(CF_3SO_3)_2$ whereas complex **3**$(CF_3SO_3)_2$ displays a lesser reactivity. The different DNA-cleavage activity of complexes **1**−**3** is due the different electronic factors and complex topology induced by the natures of the different ligands. This work constitutes an example of how small modifications introduced in the macrocyclic backbone of the metal complexes lead to dramatic changes in the nuclease activity.

Introduction

In the past few years, artificial nucleases have been presented as valuable tools in genomic research, as well as promising candidates for application in cancer therapy.[1] In this context a large number of transition metal complexes (Fe, Cu, Ni, Pt, Ru, Rh, V, Cr, Co, Mn, Os, and Pd) have been reported to mediate DNA reactions by themselves or assisted by both oxidation or reducing agents.[2] In this line lower oxidation state transition metals have been used in combination of oxygen or other forms of reactive oxygen such a hydrogen peroxide or alkylhydroperoxides to generate reactive species that damage DNA by direct strand scission or base modification.[3]

The reactivity of a metal complex will depend obviously on the nature of the metal complex as well as in the potential supramolecular interactions it can have with the DNA.[4] Copper is a biologically relevant transition metal, and its complexes are of particular interest because they possess biologically accessible redox potentials and they are typically used, upon association with dioxygen or hydrogen peroxide, for efficient and, in some instances, selective DNA cleavage through oxidative pathways.[5−8] In the past few years, multinuclearity has been one of the successful strategies to increase the efficiency and selectivity of the metallonucleases due to the potential cooperative effects between the metal centers.[2,9−11] Karlin and co-workers have already

*To whom correspondence should be addressed. E-mail: angeles.martinez@udg.edu (M.A.M.); allobet@iciq.es (A.L.).

(1) Steinreiber, J.; Ward, T. R. *Coord. Chem. Rev.* **2008**, *252*, 751–766.
(2) Jiang, Q.; Xiao, N.; Shi, P.; Zhu, Y.; Guo, Z. *Coord. Chem. Rev.* **2007**, *251*, 1951–1972.
(3) (a) Pogozelski, W. K.; Tullius, T. D. *Chem. Rev.* **1998**, *98*, 1089–1107. (b) Burrows, C. J.; Muller, J. G. *Chem. Rev.* **1998**, *98*, 1109–1151.
(4) Ronconi, L.; Sadler, P. J. *Coord. Chem. Rev.* **2007**, *251*, 1633–1648.
(5) Mirica, L. M.; Ottenwaelder, X.; Stack, D. P. *Chem. Rev.* **2004**, *104*, 1013–1045.
(6) Hatcher, L. Q.; Karlin, K. D. *J. Biol. Inorg. Chem.* **2004**, *9*, 669–683.
(7) Thyagarajan, S.; Murthy, N. N.; Narducci Sarjeant, A. A.; Karlin, K. D.; Rokita, S. E. *J. Am. Chem. Soc.* **2006**, *128*, 7003–7008.
(8) Fernandez, M. J.; Wilson, B.; Palacios, M.; Rodrigo, M. M.; Grant, K. B.; Lorente, A. *Bioconjugate Chem.* **2007**, *18*, 121–129.
(9) (a) Fang, Y.-G.; Zhang, J.; Chen, S.-Y.; Jiang, N.; Lin, H.-H.; Zhang, Y.; Yu, X.-Q. *Bioorg. Med. Chem.* **2007**, *15*, 696–701. (b) Zhao, Y.; Zhu, J.; He, W.; Yang, Z.; Zhu, Y.; Li, Y.; Zhang, J.; Guo, Z. *Chem.—Eur. J.* **2006**, *12*, 6621–6629. (c) Humphreys, K. J.; Karlin, K. D.; Rokita, S. E. *J. Am. Chem. Soc.* **2002**, *124*, 6009–6019. (d) Tu, C.; Shao, Y.; Gan, N.; Guo, Z. *Inorg. Chem.* **2004**, *43*, 4761–4766.
(10) Chen, J.; Wang, X.; Shao, Y.; Zhu, J.; Zhu, Y.; Li, Y.; Xu, Q.; Guo, Z. *Inorg. Chem.* **2007**, *46*, 3306–3312.
(11) García-Giménez, J. L.; Alzuet, G.; González-Alvarez, M.; Castiñeiras, A.; Liu-González, M.; Borrás, J. *Inorg. Chem.* **2007**, *46*, 7178–7188.

 Published on Web 11/02/2009

Scheme 1. Synthetic Scheme for Ligands and Complexes

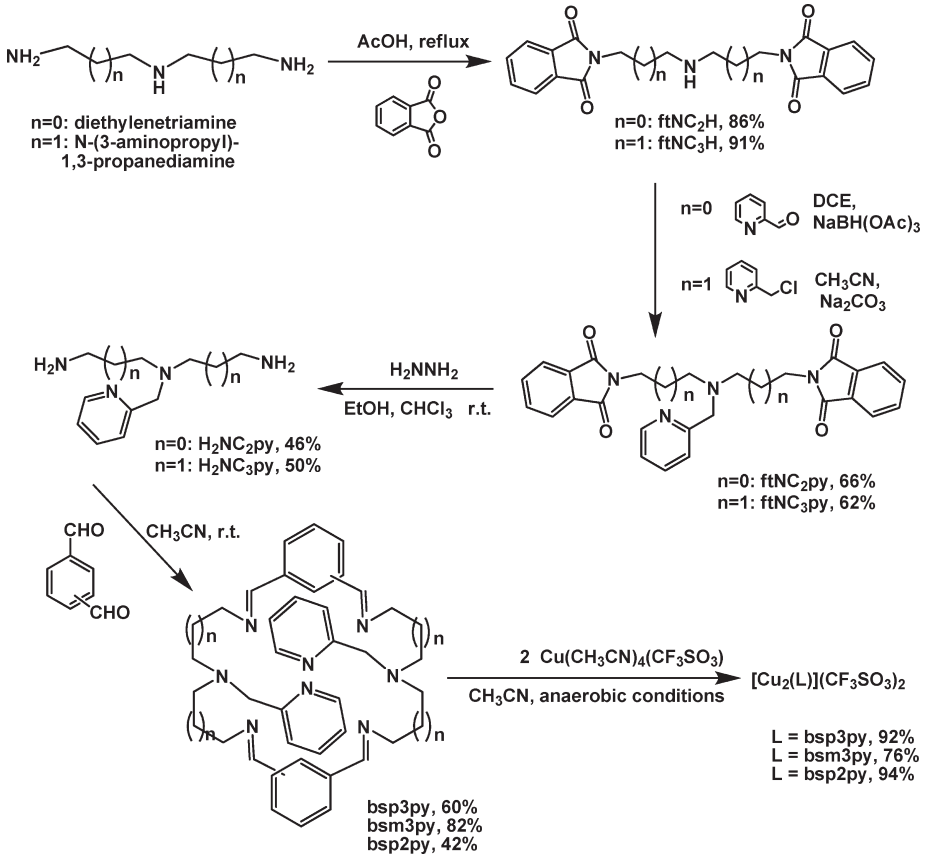

demonstrated that multinuclear Cu complexes containing pyridyl ligands have more effective cleavage abilities than their mononuclear analogues.[12] Recently, the well established properties of another series of dicopper complexes $[Cu_2(Nn)(O_2)]^{+2}$ (n = 3−5) using the dinucleating ligands Nn, in which two tridentate PY2 units (PY2 = bis[2-(2-pyridyl)-ethyl]amine) are connected by alkyl chains of varying length n, have shown a certain correlation between Cu_2-O_2 structure and DNA oxidation.[7] Nevertheless, the origin of these differences and the nature of the reactive intermediate(s) initiating the cleavage still remain unclear not only for these dinuclear complexes but also for other Cu-based nucleases in general.[13] Thus there is a need to design new DNA cleavage agents, to be able to understand structure−activity relationships as well as their mechanisms.[14] Along this line, Schiff base polyamine macrocycles can be easily used to prepare synthetically versatile ligands, and their complexes can be used to mimic enzyme actives.[15]

Here we wish to report the synthesis, structure, and spectroscopic properties of a new series of hexaazamacrocyclic ligands (see Scheme 1) containing pyridyl pendant arms together with their respective dinuclear Cu(I) complexes **1**−**3**. We were interested in exploring the possibility of these copper(I) complexes to act as artificial nucleases due to the peculiar characteristics of ligands: (i) the existence of cyclic planar aromatic and/or heterocyclic ring systems capable of being inserted or stacked between base pairs in the hydrophobic interior of helical double stranded DNA, (ii) the presence of nitrogen atoms that can establish hydrogen bonds with the DNA, and (iii) the capacity to yield dicationic dinuclear copper(I) complexes where the positive global charge could favor their electrostatic attraction to the anionic phosphate backbone of DNA. Moreover, the presence of two centers Cu(I) in the same compound could have a cooperative effect on its potential biological activity.

In these complexes the metal−metal relative disposition and the redox potential of metal ions can be finely tuned by those macrocyclic ligands. We also report the interaction of complexes **1**−**3** with DNA studied by circular dichroism (CD), atomic force microscopy (AFM), and electrophoretic mobility (EM).

(12) (a) Humphreys, K. J.; Karlin, K. D.; Rokita, S. E. *J. Am. Chem. Soc.* **2001**, *123*, 5588–5589. (b) Humphreys, K. J.; Karlin, K. D.; Rokita, S. E. *J. Am. Chem. Soc.* **2002**, *124*, 8055–8066. (c) Li, L.; Murthy, N. N.; Tesler, J.; Zakharov, L. N.; Yap, G. P. A.; Rheingold, A. L.; Karlin, K. D.; Rokita, S. *Inorg. Chem.* **2006**, *45*, 7144–7159.

(13) (a) Meijler, M. M.; Zelenco, O.; Sigman, D. S. *J. Am. Chem. Soc.* **1997**, *119*, 1135. (b) Thederahn, T. B.; Kuwabara, M. D.; Larsen, T. A.; Sigman, D. S. *J. Am. Chem. Soc.* **1989**, *111*, 4941. (c) Marshall, L. E.; Graham, D. R.; Reich, K. A.; Sigman, D. S. *Biochemistry* **1981**, *20*, 244.

(14) Zhu, Q.; Lian, Y.; Thyagarajan, S.; Rokita, S. E.; Karlin, K. D.; Blough, N. V. *J. Am. Chem. Soc.* **2008**, *130*(20), 6304–6305.

(15) (a) Lehn, J.-M. *Supramolecular Chemistry*; VCH: New York, 1995. (b) Martell, A. E. *Oxigen Complexes and Oxigen Activacion by Transition Metals*; Plenum: New York, 1988. (c) Zang, V.; van Eldik, R. *Inorg. Chem.* **1990**, *29*, 4463. (d) Franz, K. J.; Lippard, S. J. *J. Am. Chem. Soc.* **1999**, *121*, 10594. (e) Hosseini, M. W.; Lehn, J.-M; Mertes, M. P. *Helv. Chim. Acta* **1983**, *66*, 2454. (f) Bencini, A.; Bianchi, A.; Scott, E. C.; Morales, M.; Wang, B.; Garcia-España, E.; Deffo, T.; Takusagawa, F.; Mertes, M. P.; Mertes, K.-B.; Paoletti, P. *Bioorg. Chem.* **1992**, *20*, 8. (g) Izatt, R. M.; Pawlak, K.; Bruening, R. L. *Chem. Rev.* **1995**, *95*, 2529. (h) Formica, M.; Fusi, V.; Micheloni, M.; Pontellini, R.; Romani, P. *Coord. Chem. Rew.* **1999**, *184*, 347–363. (i) Sun, X.; Wuest, M.; Weisman, G. R.; Wong, E. H.; Reed, D. P.; Boswell, C. A.; Motekaitis, R.; Martell, A. E.; Welch, M. J.; Anderson, C. J. *J. Med. Chem.* **2002**, *45*, 469–477. (j) Anda, C.; Martinez, M. A.; LLobet, A. *Supramol. Chem.* **2005**, *17*(3), 257–266. (k) Arbuse, A.; Anda, C.; Martinez, M. A.; Pérez-Mirón, J.; Jaime, C.; Parella, T.; Llobet, A. *Inorg. Chem.* **2007**, *46*, 10632–10638.

Experimental Section

Physical Methods. IR spectra of solid samples were taken in a Mattson-Galaxy Satellite FT-IR spectrophotometer using a MKII Golden Gate single reflection ATR system. IR solution experiments were performed on a FTIR spectrometer Thermo Nicolet 5700, with DLaTGS and MCT detectors with KBr windows Omnicell from Specac. UV−vis spectroscopy was performed on a Cary 50 Scan (Varian) UV−vis spectrophotometer with 1 cm quartz cells.

NMR spectra were taken on a Bruker DPX 200 MHz. Elemental analyses were performed using a CHNS-O EA-1108 elemental analyzer from Fisons. The ESI-MS experiments were performed on a Navigator LC/MS chromatograph from Thermo Quest Finigan, using acetonitrile as a mobile phase. Square wave voltammetry experiments were performed in an IJ-Cambria HI-660 potentiostat using a three electrode cell. Glassy carbon disk electrodes (3 mm diameter) from BAS were used as working electrode, platinum wire was used as auxiliary, and SSCE was used as the reference electrode.

Materials and Synthesis. The reagents and solvents used were of commercially available reagent quality unless otherwise stated. Solvents were purchased from SDS. Acetonitrile, pentane, and CH_2Cl_2 were distilled over CaH_2 under nitrogen. Preparation and manipulation of Cu(I) complexes were carried out in a N_2 drybox (Braun) with O_2 and H_2O concentrations < 1.0 ppm. calf thymus DNA (CT DNA), EDTA (ethylene-diamino tetracetic acid), and Tris-HCl (tris-(hydroxymethyl)aminomethane-hydrochloride) used in the CD study were obtained from Sigma (Madrid, Spain). pBR322 plasmid DNA used in the EM and AFM studies were obtained from Boehringer Mannheim (Germany). Ultrapure agarose was obtained from ECOGEN (Barcelona, Spain). HEPES (*N*-2-hydroxyethyl piperazine-*N*′-2-ethanesulfonic acid) was obtained from ICN (Madrid).

Ligand Synthesis. 1,7-Diphthalimido-4-azaheptane (ftNC$_3$H). This compound was synthesized by a procedure similar to that described for **ftNC$_2$H** (see below), but using *N*-(3-aminopropyl)-1,3-propanediamine (14.3 mL, 0.1 mol) and phthalic anhydride (33.2 g, 0.2 mol) in 160 mL of glacial acetic acid. Yield: 35.54 g (91%). ^{1}H NMR (200 MHz, $CDCl_3$) δ (ppm): 1.92 (quint, J = 6 Hz, 4H, Hb), 2.73 (t, J = 6 Hz, 4H, Ha), 3.75 (t, J = 6 Hz, 4H, Hc), 7.64−7.82 (m, 8H, arom). FT-IR ν (cm^{-1}): 1701 (C═O), 1395 (CO—N), 718 (C—H ft), 531 (C−H ft).

4-(2-Pyridylmethyl)-1,7-diphthalimido-4-azaheptane (ftNC$_3$py). A mixture of **ftNC$_3$H** (9.85 g, 0.025 mol), 2-(chloromethyl)pyridine hydrochloride (5.01 g, 0.030 mol), Na_2CO_3 (6.58 g, 0.062 mol), and 150 mg of tetrabutylammonium bromide in 450 mL of acetonitrile was refluxed for 48 h. The solvent was then evaporated, and the dry residue was treated with H_2O and extracted with dichloromethane (3 × 100 mL). This extract was dried with anhydrous $MgSO_4$ and evaporated to give a solid, which was recrystallized in methanol. Yield: 7.59 g (62%). ^{1}H NMR (200 MHz, $CDCl_3$) δ (ppm): 1.83 (quint, J = 7 Hz, 4H, Hb), 2.56 (t, J = 7 Hz, 4H, Ha), 3.70 (s, 2H, Hd), 3.70 (t, J = 7 Hz, 4H, Hc), 7.0−7.1 (m, 1H, Hβ), 7.4−7.8 (m, 10H, arom + Hβ' + Hγ), 8.35−8.45 (m, 1H, Hα). FT-IR ν (cm^{-1}): 1702 (C═O), 1590 (C═C py), 1467 (C═C), 1396 (CO—N), 753 (C—H py), 716 (def C—H ft), 614 (C—H py), 530 (def C—H ft). MS (m/z): 483.3 (MH$^+$). Anal. Calcd (%) for $C_{28}H_{26}N_4O_4\cdot 0.5H_2O$ (MW = 491.54 g·mol^{-1}): C, 68.42; N, 11.40; H, 5.54. Found: C, 68.50; N, 11.42; H, 5.76.

5-(2-Pyridylmethyl)-1,5,9-triazanonane (H$_2$NC$_3$py). A mixture of **ftNC$_3$py** (3,67 g, 7.57 mmol) and hydrazine monohydrate (5.0 mL, 100 mmol) in 170 mL of ethanol and 35 mL of chloroform was allowed to react at room temperature for 24 h. The white solid was then filtered off, and the filtrate was evaporated under reduced pressure. A total of 150 mL of chloroform was added, and the solution was stirred for 24 h more, then filtered again, and evaporated to dryness to obtain a product as a yellow oil. Yield: 0.85 g (50%). ^{1}H NMR (200 MHz, $CDCl_3$) δ (ppm): 1.2−1.5 (4H, NH_2), 1.59 (quint, J = 7 Hz, 4H, Hb), 2.50 (t, J = 7 Hz, 4H, Ha), 2.68 (t, J = 7 Hz, 4H, Hc), 3.68 (s, 2H, Hd), 7.00−7.15 (m, 1H, Hβ), 7.35−7.45 (m, 1H, Hβ'), 7.50−7.70 (m, 1H, Hγ), 8.0−8.5 (m, 1H, Hα). FT-IR ν (cm^{-1}): 3362, 3285 (NH_2), 2930, 2855, 2812 (C—H), 1589 (C═C py), 1568 (—NH_2), 1471, 1432 (—CH_2—), 755 (def C—H py), 615 (C—H py).

1,5-Diphthalimido-3-azapentane (ftNC$_2$H). This compound was obtained as described in the literature[16] using diethylenetriamine (11.20 mL, 0.1 mol), phthalic anhydride (30.54 g, 0.2 mol), and 160 mL of acetic acid. Yield: 31.25 g (86%). ^{1}H NMR (200 MHz, $CDCl_3$) δ (ppm): 1.50 (s, 1H, N−H), 3.00 (t, J = 6 Hz, 4H, Ha), 3.81 (t, J = 6 Hz, 4H, Hc), 7.6−7.8 (m, 8H, arom). FT-IR ν (cm^{-1}): 3328 (N−H), 2943, 2868 (C—H), 1702 (C═O), 1393 (CO—N), 716 (C—H ft), 531 (C—H ft).

3-(2-Pyridylmethyl)-1,5-diphthalimido-3-azapentane (ftNC$_2$py). A mixture of **ftNC$_2$H** (10.00 g, 0.0275 mol), 2-pyridinecarboxaldehyde (2.65 mL, 0.0275 mol), and sodium triacetoxyborohydride (8.52 g, 0.040 mol) in 100 mL of 1,2-dichloroethane was stirred under nitrogen atmosphere for 12 h. Then 100 mL of 2 M NaOH solution was added. The organic layer was extracted, and the aqueous phase was washed with 100 mL of dichloromethane twice. The extract was dried over sodium sulfate and evaporated to dryness. The product was purified through recrystallization with methanol. Yield: 8.21 g (66%). ^{1}H NMR (200 MHz, $CDCl_3$) δ (ppm): 2.83 (t, J = 6 Hz, 4H, Ha), 3.75 (t, J = 6 Hz, 4H, Hc), 3.83 (s, 2H, Hd), 6.8−7.0 (M, 1H, Hβ), 7.0−7.2 (m, 2H, Hβ' + Hγ), 7.6−7.8 (m, 8H, arom), 8.3−8.4 (m, 1H, Hα). FT-IR ν (cm^{-1}): 1699 (C═O), 1592 (C═C py), 1466 (C═C), 1433 (—CH_2—), 1394 (CO—N), 756 (C—H py), 714 (C—H ft), 616 (C—H py), 529 (C—H ft). Anal. Calcd (%) for $C_{26}H_{22}N_4O_4\cdot 0.6\ H_2O$ (MW = 465.29 g·mol^{-1}): C, 67.12; N, 12.04; H, 5.03. Found: C, 67.30; N, 12.09; H, 5.42.

4-(2-pyridylmethyl)-1,4,7-triazaheptane (H$_2$NC$_2$py). The procedure was analogous to that used for the deprotection of **ftNC$_3$py**, using **ftNC$_2$py** (10.00 g, 0.022 mol) and hydrazine hydrate (14.0 mL, 0.283 mol) in 500 mL of ethanol and 100 mL of chloroform. Yield: 1.96 g (46%). ^{1}H NMR (200 MHz, $CDCl_3$) δ (ppm): 2.63 (t, J = 6 Hz, 4H, Ha), 2.82 (t, J = 6 Hz, 4H, Hc), 3.79 (s, 2H, Hd), 7.1−7.2 (m, 1H, Hβ), 7.4−7.5 (m, 1H, Hβ'), 7.6−7.7 (m, 1H, Hγ), 8.55−8.65 (m, 1H, Hα). FT-IR ν (cm^{-1}): 3353, 3279 (NH_2), 2936, 2861 (C—H), 1591 (C═C py), 1474, 1433 (—CH_2—), 758 (C—H py), 614 (def C—H py).

7,22-(2-Pyridylmethyl)-3,7,11,18,22,26-hexaazatricyclo[26.2.2.2^{13,16}]tetratiaconta-1(31),2,11,13,15,17,26,28(32),29,33-decaene (bsp3py). To a solution of **H$_2$NC$_3$py** (0.30 g, 1.3 mmol) in 18 mL of acetonitrile was added, slowly and under an ice bath, a solution of terephthalaldehyde (0.18 g, 1.3 mmol) in 18 mL of acetonitrile. The mixture was stirred over 12 h at room temperature, precipitating a colorless oil. The solution was decanted, and the oil dried to vacuum, turning into a white solid. Yield 0.26 g (60%). ^{1}H NMR (200 MHz, $CDCl_3$) δ (ppm): 1.88 (quint, J = 7 Hz, 8H, Hb), 2.61 (t, J = 7 Hz, 8H, Ha), 3.64 (t, J = 7 Hz, 8H, Hc), 3.77 (s, 4H, Hd), 7.1−7.3 (m, 2H, Hβ), 7.4−7.8 (m, 12H, arom + Hβ + Hγ), 8.22 (s, 4H, He), 8.5−8.6 (m, 2H, Hα). FT-IR ν (cm^{-1}): 2970, 2927, 2871, 2839, 2796 (C—H), 1640 (C═N), 1590, 1568 (C═C py), 1476, 1431 (—CH_2), 826 (C—H ar), 750 (def C—H py), 618 (C—H py). MS (m/z): 641.2 (MH$^+$).

7,23-(2-Pyridylmethyl)-3,7,11,19,23,27-hexaazatricyclo[27.3.1.1^{13,17}]tetratiaconta-1(32),2,11,13,15,17(34),18,27,29(33),30-decaene (bsm3py). The procedure was analogous to that used for the synthesis of **bsp3py**, using **H$_2$NC$_3$py** (1.88 g, 8.5 mmol) in 85 mL of acetonitrile and isophthalaldehyde (1.17 g, 8.5 mmol) in 85 mL of acetonitrile. Yield: 2.22 g (82%). ^{1}H NMR (200 MHz,

(16) Martell, A. E.; Motekaitis, R. J; Yuen Ng, C. *Inorg. Chem.* **1979**, *18*, 2982–2986.

(17) Mier-Vinué, J.; Lorenzo, J.; Montaña, A. M.; Moreno, V.; Avilés, F. X. *J. Inorg. Biochem.* **2008**, *102*, 973–987.

$CDCl_3$) δ (ppm): 1.88 (quint, J = 7 Hz, 8H, Hb), 2.6 (t, J = 7 Hz, 8H, Ha), 3.65 (t, J = 7 Hz, 8H, Hc), 3.76 (s, 4H, Hd), 7.00−7.9 (m, 14H, 8Har + 2Hβ' + 2Hγ + 2Hβ), 8.24 (s, 4H, He), 8.4−8.6(m, 2H, Hα). FT-IR ν (cm^{-1}): 2927, 2835 (C—H), 1644 (C=N), 1590 (C=C py), 1434 (—CH_2—), 798 (C—H ar), 757 (C—H py), 691 (C—H ar), 616 (C—H py). MS (m/z): 641.2 (MH^+).

6,19-(2-Pyridylmethyl)-3,6,9,16,19,22-hexaazatricyclo[22.2.2.$2^{11,14}$]triaconta-1(27),2,9,11(30),12,14(29)15,22,24(28),25-decaene (bsp2py). The synthesis of **bsp2py** was analogous to the synthesis of **bsp3py**, using H_2NC_2py (1.03 g, 5.32 mmol) in 53 mL of acetonitrile and terephthalaldehyde (0.71 g, 5.32 mmol) in 53 mL of acetonitrile. Yield: 0.65 g (42%). ^{1}H NMR (200 MHz, $CDCl_3$) δ (ppm): 2.97 (t, J = 7 Hz, 8H, Ha), 3.77 (t, J = 7 Hz, 8H, Hc), 3.85 (s, 4H, Hd), 7.1−7.3 (m, 2H, Hβ), 7.4−7.8 (m, 12H, 8 Harom + 2Hγ + 2Hβ'), 8.22 (s, 4H, He), 8.5−8.6 (m, 2H, Hα). FT-IR ν (cm^{-1}): 2924, 2838 (C—H), 1642 (C=N), 1589, 1568 (C=C py), 1432 (—CH_2—), 828 (C—H ar), 756 (C—H py). MS (m/z): 585.3 (MH^+).

Synthesis of Complexes. $[Cu_2^I(L)](CF_3SO_3)_2$ (L = **bsp3py**, **bsm3py**, **bsp2py**) were prepared by the same general method in an anaerobic box, adding a solution of $Cu^I(CH_3CN)_4(CF_3SO_3)$ (0.040 g, 0.106 mmol) in CH_3CN (1 mL) to a suspension of particular ligand (0.034 g for **bsp3py** and **bsm3py**, 0.029 g for **bsp2py**, 0.053 mmol) in CH_3CN (1 mL). The corresponding reaction mixture was stirred for 1−2 h. Addition of diethyl ether causes the precipitation of the resulting complex, which was isolated by decantation and dried under vacuum.

$[Cu_2^I(L)](BArF)_2$ (L = **bsp3py**, **bsm3py**, **bsp2py**) were prepared, with the purpose of improving the solubility of the complexes in CH_2Cl_2, as follows: to a suspension of 0.040 mmol of the corresponding triflate complex (0.043 g for **1(CF$_3$SO$_3$)$_2$** and **2(CF$_3$SO$_3$)** and 0.040 g for **3(CF$_3$SO$_3$)$_2$**) in dicholoromethane, 0.072 g of NaBArF (0.080 mmol) is added. The suspension is stirred for 3−4 h and then filtered so that the $NaCF_3SO_3$ is filtered off. Then 5 mL of pentane are added carefully so that it does not mix with the dicholomethane. Twenty-four hours later, decantation of the liquid and drying of the obtained solid lead to the pure BArF complexes.

$[Cu_2^I$(bsp3py)](CF$_3$SO$_3$)$_2$ (1(CF$_3$SO$_3$)$_2$). The product resulted in 0.052 g (92% yield) of a red solid. Single crystals of **1(CF$_3$SO$_3$)$_2$** suitable for X-ray diffraction analysis were obtained by slow diethyl ether diffusion into acetonitile solution of the complex. Anal. Calcd (%) for $C_{42}H_{48}Cu_2F_6N_8O_6S_2 \cdot 1.5\ H_2O$ (MW = 1093.11 g·mol^{-1}): C, 46.15; N, 10.25; H, 4.70, S, 5.87. Found: C, 46.02; N, 10.02; H, 4.60, S, 5.71.

^{1}H NMR (400 MHz, DMSO-d_6) δ (ppm): the corresponding spectre is identical to that obtained in a DMSO-d_6−D_2O (1:4) mixture.

^{1}H NMR (400 MHz, DMSO-d_6−D_2O (1:4)) δ (ppm): 1.7−1.9 (m, 4H, Hb(1)), 2.0−2.1 (m, 4H, Hb(2)), 2.5−2.7 (m, 4H, Ha(1)), 2.9−3.1 (m, 4H, Ha(2)), 3.4−3.6 (m, 4H, Hc(1)), 3.78 (s, 4H, Hd), 3.9−4.0 (m, 4H, Hc(2), 7.53 (s, 8H, Har), 7.6−7.7 (m, 4H, Hβ), 7.9−8.0 (m, 2H, Hγ), 8.37 (s, 4H, N=CH), 8.6−8.7 (m, 2H Hα).

^{13}C NMR (100 MHz, DMSO-d_6) δ (ppm): 27.7 (Cb), 58.1 (Ca), 60.0 (Cd), 64.1 (Cc), 125.1 (Cβ), 127.9 (*C*-Har), 137.2 (Cq, ar), 138.5 (Cγ), 149.0 (Cα), 157.7 (Cα), 164.0 (*C*=NH).

ESI-MS in aqueous DMSO (m/z): 917.2 $[Cu_2L](OTf)^+$. $E_{1/2}$(MeCN) = 0. 82 V vs SSCE.

$[Cu_2^I$(bsp3py)](BArF)$_2$ (1(BArF)$_2$). The product resulted in 0.078 g (78% Yield) of an orange solid. Anal. Calcd (%) for $C_{104}H_{72}B_2Cu_2F_{48}N_8 \cdot 2H_2O$ (MW = 2530.41 g·mol^{-1}): C, 49.37; N, 4.43; H, 3.03. Found: C, 49.40; N, 4.64; H, 3.04.

^{1}H NMR (200 MHz, CH_3CN) δ (ppm): 1.8−2.0 (m, 4H, Hb(1)), 2.0−2.2 (m, 4H, Hb(2)), 2.6−2.8 (m, 4H, Ha(1)), 3.0−3.2 (m, 4H, Ha(2)), 3.5−3.7 (m, 4H, Hc(1)), 3.81 (s, 4H, py—CH_2—N—), 3.9−4.1 (m, 4H, Hc(2)), 7.4−7.8 (m, 36H, 24H$_{BArF}$ + 8Harom + 4Hβ), 7.9−8.0 (m, 2Hγ), 8.27 (s, 4H, N=CH—), 8.6−8.8 (m, 2Hα).

$[Cu_2^I$(bsm3py)](CF$_3$SO$_3$)$_2$ (2(CF$_3$SO$_3$)$_2$). The product resulted in 0. 043 g (76% yield) of a dark red solid. Anal. Calcd (%) for $C_{42}H_{48}Cu_2F_6N_8O_6S_2$ (MW = 1066.09 g·mol^{-1}): C, 47.32; N, 10.51; H, 4.54, S, 6.02. Found: C, 47.59; N, 10.74; H, 4.70, S, 5.29.

^{1}H NMR (400 MHz, DMSO-d_6) δ (ppm): 1.7−2.0 (m, 8H, Hb), 2.5−2.7 (m, 8H, Ha), 3.2−4.0 (m, 12H, 8Hc + 4H py—CH_2—N), 7.4−8.1 (m, 12 H, 6Harom + 6H$_{py}$), 8.6−9.0 (m, 6H, Hα_{py} + 4N=CH—), 9.40 (s, 2Har).

^{1}H NMR (400 MHz, DMSO-d_6−D_2O) δ (ppm): 1.7−2.0 (m, 8H, Hb), 2.4−2.8 (m, 8H, Ha), 3.1−3.5 (m, 8H, Hc), 3.8−4.2 (m, 4H, py—CH_2—N), 7.3−8.0 (m, 12 H, 6Harom + 6Hpy), 8.5−8.9 (m, 6H, 2Hα_{py} + 4H, N=CH-), 9.40 (s, 2Har).

^{13}C NMR (100 MHz, DMSO-d_6) δ (ppm): 28.9 (Cb), 59.4 (Ca), 63.8 (Cc + py—CH$_2$—N), 119.0 (C$_{ar,quat}$), 123.1 (Cβ_{py}), 123.3 (Cβ_{py}), 138.7 (Cγ_{py}), 149.3 (Cα_{py}), 158.2 N=*C*H—).

$E_{1/2}$(MeCN) = 0.89 V vs SSCE.

$[Cu_2^I$(bsm3py)](SbF$_6$)$_2$ (2(SbF$_6$)$_2$). Compound **2(SbF$_6$)$_2$** was obtained by reacting **bsm3py** with $Cu^I(CH_3CN)_4(SbF_6)$ in CH_3CN using the same general method for **2(CF$_3$SO$_3$)$_2$**. Slow diethyl ether diffusion in an acetonitrile solution of **2(SbF$_6$)$_2$** complexes afforded brownish crystals suitable for X-ray diffraction.

$[Cu_2^I$(bsm3py)](BArF)$_2$ (2(BArF)$_2$). The product resulted in 0.065 g (64% yield) of an orange solid. Anal. Calcd (%) for $C_{104}H_{72}B_2Cu_2F_{48}N_8$ (MW = 2494.38 g·mol^{-1}): C, 50.09; N, 4.49; H, 2.91. Found: C, 49.76; N, 4.68; H, 3.05.

^{1}H NMR (200 MHz, CD_2Cl_2) δ (ppm): 1.8−2.2 (m, 8H, Hb), 2.5−3.0 (m, 8H, Ha), 3.4−4.0 (m, 12H, 8Hc + 4H py—CH_2—N), 7.2−8.6 (m, 44 H, 24H$_{BArF}$ + 8Harom + 8Hpy + 4N=CH—).

ESI-MS (m/z): 1631.3 $[Cu_2L](BArF)^+$.

$[Cu_2^I$(bsp2py)](CF$_3$SO$_3$)$_2$ (3(CF$_3$SO$_3$)$_2$). The product resulted in 0.053 g (94% yield) of a reddish orange solid. Slow diethyl ether diffusion in an acetonitile solution of complex led to the formation of single crystals of **3(CF$_3$SO$_3$)$_2$** suitable for X-ray analysis. Anal. Calcd (%) for $C_{38}H_{40}Cu_2F_6N_8O_6S_2 \cdot 2.5H_2O$ (MW = 1055.03 g·mol^{-1}): C, 43.26; N, 10.62; H, 4.30; S, 6.08. Found: C, 43.20; N, 10.50; H, 4.05; S, 6.02.

^{1}H NMR (400 MHz, DMSO-d_6) δ (ppm): the corresponding spectre is identical to that obtained in a DMSO-d_6−D_2O (1:4) mixture.

^{1}H NMR (400 MHz, DMSO-d_6−D_2O (1:4)) δ (ppm): 2.9−3.0 (m, 4H, Ha(1)), 3.3−3.4 (m, 4H, Ha(2)), 3.75−3.85 (m, 4H, Hc(1)), 3.95−4.1 (m, 4H, Hc(2)), 4.40 (s, 4H, Hd), 7.4−7.5 (m, 2H, Hβ), 7.55−7.65 (m, 2H, Hβ), 7.9−8.0 (m, 2H, Hγ), 8.56 (s, 8H, Har), 8.67 (s, 4H, N=CH), 8.8−8.9 (m, 2H, Hα).

^{13}C NMR (100 MHz, DMSO-d_6) δ (ppm): 52.4 (Cc), 57.2 (Cd), 59.9 (Ca), 124.2, 124.3 (Cβ), 128.5 (*C*Har), 136.5 (Cq ar), 138.0 (Cγ), 149.3 (*C*Hα), 158.8 (*C*Hα), 161.8 (N=*C*H).

ESI-MS in aqueous DMSO: (m/z): 861.1 $[Cu_2L](OTf)^+$. $E_{1/2}$(MeCN) = 0.71 V vs SSCE.

$[Cu_2^I$(bsp2py)](BArF)$_2$ (3(BArF)$_2$). The product resulted in 0.069 g (71% yield) of an orange solid. Anal. Calcd (%) for $C_{100}H_{64}B_2Cu_2F_{48}N_8 \cdot 3H_2O$ (MW = 2492.31 g·mol^{-1}): C, 45.30; N, 4.36; H, 2.52. Found: C, 45.54; N, 4.21; H, 2.65.

^{1}H NMR (200 MHz, CH_2Cl_2) δ (ppm): 3.0−3.2 (m, 4H, Ha(1)), 3.3−3.5 (m, 4H, Ha(2)), 3.7−3.9 (m, 4H, Hc(1)), 3.9−4.2 (m, 4H, Hc(2)), 5.30 (s, 4H, py—CH_2—N—), 7.0−8.5 (m, 34 H, 24H$_{BArF}$ + 8Harom + 8Hpy + 4N=CH—).

^{1}H NMR (200 MHz, CH_3CN) δ (ppm): 2.9−3.3 (m, 8H, Ha), 3.8−4.1 (m, 8H, Hc), 4.3−4.5 (m, 4H, Hd), 7.0−8.5 (m, 44 H, 24H$_{BArF}$ + 8Harom + 8Hpy + 4N=CH—).

Solubility and Stability. The copper complexes were soluble in DMSO and aqueous DMSO. The binuclear complexes were found to be stable in the solution phases used, as evidenced by the NMR.

X-ray Diffraction Studies. Crystals of **1(CF$_3$SO$_3$)$_2$**, **2(SbF$_6$)$_2$**, and **3(CF$_3$SO$_3$)$_2$** were respectively mounted on a nylon loop and

Table 1. Crystallographic data for $\mathbf{1}(CF_3SO_3)_2$, $\mathbf{2}(SbF_6)_2$ and $\mathbf{3}(CF_3SO_3)_2$[a]

	complex		
	$\mathbf{1}(CF_3SO_3)_2$	$\mathbf{2}(SbF_6)_2$	$\mathbf{3}(CF_3SO_3)_2$
empirical formula	$C_{46}H_{58}Cu_2F_6\ N_8O_7S_2$	$C_{42}H_{51}Cu_2F_{12}N_9Sb_2$	$C_{40}H_{43}Cu_2F_6N_9O_6$
formula weight	1140.20	1280.50	1051.03
temperature, K	100(2)	100(2)	100(2)
wavelength, Å	0.71073	0.71073	0.71073
crystal system	monoclinic	monoclinic	triclinic
space group	$P21/n$	$P21/c$	$P\bar{1}$
a, Å	19.833(6)	11.9994(9)	10.7658(11)
α, deg	90	90	110.323(2)
b, Å	12.470(4)	24.7847(18)	13.4453(14)
β, deg	111.172(5)	90	94.852(2)
c, Å	21.921(6)	16.6745(12)	16.5660(17)
γ, deg	90	90	98.578(2)
volume, Å^3	5055(3)	4931.7(6)	2199.3(4)
Z	4	4	2
ρ (g/cm^3)	1.498	1.725	1.587
$R\ [I > 2\sigma(I)]^{\alpha}$	0.0797	0.0473	0.0568
wR	0.2612	0.1230	0.1155

[a] $R = \sum[F_o - F_c]/\sum F_0$; $wR = [\sum(w(F_o^2 - F_c^2)^2)/\sum(wF_o^4)]^{1/2}$.

used for low temperature (100(2) K) X-ray structure determination. The measurement were carried out on a BRUKER SMART APEX CCD diffractometer using graphite-monochromated Mo Kα radiation (λ = 0.71073 Å) from an X-ray tube. The measurements were made in the range 2.29 to 28.34° for θ. Full-sphere data collection was carried out with ω and φ scans. For $\mathbf{1(CF_3SO_3)_2}$, a total of 77 760 reflections were collected of which 12 442 [R(int) = 0.0443] were unique. For $\mathbf{2(SbF_6)_2}$ a total of 75 425 reflections were collected of which 12 135 [R(int) = 0.0379] were unique. For $\mathbf{3(CF_3SO_3)_2}$ a total of 35 011 reflections were collected of which 10 688 [R(int) = 0.0958] were unique. In all the cases, the data collection was executed using the SMART program version 5.631 (Bruker AXS 1997-02). The data reduction was made by the SAINT program + version 6.36A (Bruker AXS 2001). Absorption correction was carried out using SADABS version 2.10 (Bruker AXS 2001). Structure solution and refinement were done using SHELXTL program version 6.14 (Bruker AXS 2000−2003). For $\mathbf{2(SbF_6)_2}$ the Squeeze tool of the platon program (Spek, A. L. (2005). PLATON, A Multipurpose Crystallographic Tool, Utrecht University, Utrecht, The Netherlands) was used to remove electron density attributable to disordered solvent. The structures were solved by direct methods and refined by full-matrix least-squares methods on F^2. The non-hydrogen atoms were refined anisotropically. The H-atoms were placed in geometrically optimized positions and forced to ride on the atom to which they were attached.

Crystal data, data collection parameters, and results of the analyses are listed in Table 1.

CD Spectroscopy. All compounds were dissolved in an aqueous solution with 20% DMSO prepared with milli-Q water (4×10^{-4} M). The use of DMSO is to facilitate the dissolution of compounds to be evaluated. The stock solutions of complexes were freshly prepared before use. A stock solution (20 μg/mL) of CT DNA in TE buffer solution (50 mM NaCl, 10 mM tris-(hydroxymethyl)aminomethane hydrochloride (Tris-HCl), and 0.1 mM H_4edta, pH 7.4) was prepared and kept at 4 °C before use. The final concentration of DNA was determined by measuring the absorbance at 260 nm in a UV−vis spectrophotometer. The samples were prepared by addition of aliquot parts of the Cu-complex solutions to stock solutions of CT DNA in TE (5 mL). The amount of complex added to the DNA solution was designated as r_i (the input molar ratio of Cu to nucleotide).[17] This parameter reflects the proportion between the dicopper complex and the base pair of DNA (mol of compound/mol of nucleotide). The CD spectra of DNA in the presence or absence of Cu(I) complexes (DNA concentration 20 μg/mL, molar ratios r_i = 0.10, 0.30, 0.50) were recorded at room temperature, after 24 h incubation at 37 °C, on a JASCO J-720 spectropolarimeter with a 450 W xenon lamp using a computer for spectral subtraction and noise reduction. As a blank, a solution in TE of free native DNA was used. Each sample was scanned twice in a range of wavelengths between 220 and 330 nm. The CD spectra drawn are the average of three independent scans. The data are expressed as average residue molecular ellipticity (θ) in deg·cm^2·dmol^{-1}.

EM in Agarose Gel. pBR322 plasmid DNA of 0.25 μg/μL (8.84×10^{-8} M) concentration was used for the experiments. Stock solutions of the Cu complexes (4×10^{-4} M) in milli-Q water with 20% DMSO were freshly prepared before use. Aliquot parts of 21 μL of Cu complex solutions were added to aliquot parts of 3 μL of the pBR322 DNA in 20 μL of a TE (Tris-H_4edta, Tris-(hydroximethyl)aminomethaneethylendiaminetetracetic acid) buffer solution (50 mM NaCl, 10 mM Tris-HCl, 0.1 mM H_4edta, pH 7.4). The samples were prepared with an input molar ratio of the complex to nucleotide r_i = 6.9. The reaction mixture was incubated at 37 °C for 2 h, and then 4 μL of charge marker were added to aliquots parts of 20 μL of the adduct complex/DNA. The mixtures were electrophoretized in agarose gel (1% in TBE buffer, Tris-borate-EDTA) for 5 h at 1.5 V/cm. Afterward, the DNA was dyed with ethydium bromide solution (0.5 μg/μL in TBE) for 20 min. A sample of free DNA was used as a control. The experiment was carried out in an ECOGEN horizontal tank connected to PHARMACIA GPS 200/400 variable potential power supply.

H_2O_2 (1 μL, 33% w/v) was always added after incubation to the reaction samples prepared as described above. Samples with H_2O_2 were run at room temperature for different times (t_1 = 3 min; t_2 = 30 min) and then quenched and analyzed according to the procedures described above. A control experiment with H_2O_2 in the absence of Cu complexes was included (see Figure S19, Supporting Information).

Experiments under inert atmosphere were carried out using Schlenk techniques. Solvents for the preparation of complex solutions were degassed prior to the dissolution of the complex under nitrogen. Eppendorfs containing the DNA and buffer solutions were submitted to vacuum and left under N_2 atmosphere before the addition of the complex solution. Eppendorfs were tightly sealed with parafilm in the nitrogen atmosphere and incubated at 37 °C for 2 h.

AFM. pBR322 plasmid DNA of 0.25 μg/μL (8.84×10^{-8} M) of concentration was used for the experiments. Stock Cu complex

solutions (4×10^{-4} M) in milli-Q water with 20% DMSO were freshly prepared before use. Aliquot parts of 7 μL of these solutions were added to aliquots parts of 1 μL of the pBR322 DNA in 50 μL of a 40 mM HEPES buffer solution (HEPES (*N*-2-hydroxyethyl piperazine-*N*′-2-ethanesulfonic acid), 10 mM $MgCl_2$, pH = 7.4). The samples were prepared with an input molar ratio of the complex to nucleotide $r_i = 6.9$. The different solutions as well as Milli-Q water were passed through 0.2 nm FP030/3 filters (Scheicher & Schueell GmbH, Germany) to provide a clear background when they were imaged by AFM. The resulting solutions were incubated for 2 h at 37 °C. The samples were imaged in a Nanoscope III multimode atomic force microscope (Digital Instrumentals Inc., Santa Barbara) operating in tapping mode.

Samples were treated after incubation with 1 μL of H_2O_2 (33% w/v) for different times and then imaged according to the procedures described above.

Results

Synthesis, Structure, and Redox Properties. The macrocyclic ligands and their dicopper(I) complexes described in this work (see Chart 1) are prepared following the procedure depicted in the Scheme 1. A 2 + 2 condensation between the corresponding dialdehydes and the previously prepared diamines affords the desired ligands. To prepare the functionalized amines the initial triamines are protected with phthtalic anhydride, followed by functionalization of the central secondary amine and finally deprotecting with hydrazine in ethanol/chloroform at room temperature. The Cu(I) complexes are easily obtained by direct reaction of the ligands with Cu(I) salts. A complete structural and spectroscopic characterization is reported in the Experimental Section. The ligand **bsp2py** has already been reported by Fabrizzi et al.[18] using another strategy, although it had not been isolated neither fully characterized.

Complexes **1**$(CF_3SO_3)_2$, **2**$(SbF_6)_2$, and **3**$(CF_3SO_3)_2$ have been characterized by means of X-ray diffraction analysis, their crystallographic data is collected in the Table 1 ,and their ORTEP plots are presented in Figure 1. Bond lengths and angles for the metal coordination environment are listed in Table 2. The cationic part of the three complexes contain the macrocyclic ligands coordinating two copper atoms. Each metal center is bonded to four nitrogens of the ligand at each side of the spacer, showing a distorted tetrahedral coordination. The N_{im}—Cu and N_{py}—Cu distances are very similar ranging from 1.959(4) Å to 2.073(4) Å (see Table 2) whereas the N_{ter}—Cu distance is significantly longer in the range of 2.200(3) Å to 2.221(4) Å which is in agreement with distances previously reported for related complexes.[19−21] The geometries around the copper centers are relatively similar, although complex **3** that forms five member rings is slightly more constrained than **1** and **2** that form six member rings (see bond angles in Table 2). It is interesting to mention here that the distances between metal centers are basically controlled by the meta or para substitution in the phenylic spacer (around 7 Å for para and 4.5 Å for meta) even though in solution there will be a certain flexibility, and also influences the 3D topography of the molecule. Thus the meta molecule has a spherical shape whereas the para substituted resembles a rectangular cuboid. The methylenic spacers between the amine nitrogen atoms have a strong influence to the relative disposition of the metal centers, as has been previously shown by related macrocyclic complexes[20] that is neatly reflected by the angles between the pyridylic rings ($\theta_{py—py}$ = 50.88° for **1**, 80.36° for **2**, and 79.61° for **3**) and also but to a lesser degree to the angle between the phenylic rings (θ_{ph-ph} = 17.14° for **1**, 52.85° for **2**, and 85.51° for **3**) due to their relative rotational capacity.

Chart 1. Drawing of the Macrocyclic Ligands Together with the Abbreviations

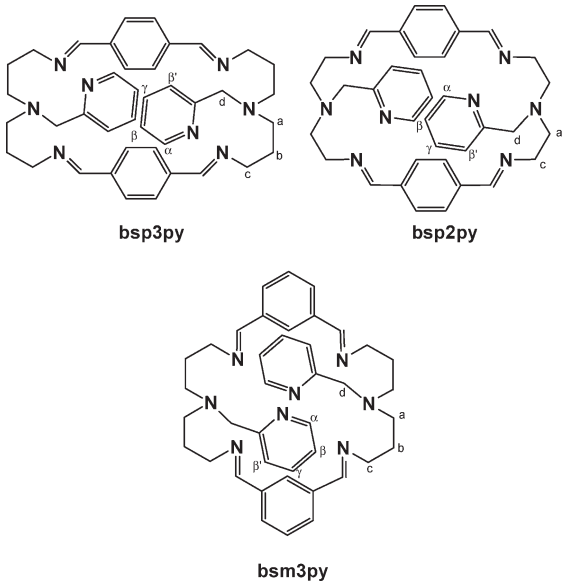

The redox properties of complexes **1**−**3** were investigated by CV and SQWV, and the voltammograms are shown in the Supporting Information. The CV of complexes **1**−**3** show chemically irreversible waves in the anodic region indicating the irreversibility of the Cu(II)/Cu(I) redox couple which is not unusual for this type of compound given the different coordination preferences of these two oxidation states of Cu. On the other hand SQWV experiments with a pulse frequency of 10 Hz allows the formal redox potentials of the Cu(II)/Cu(I) couple to be calculated, and they are 0.82, 0.89, and 0.71 V for **1**, **2**, and **3** respectively. These redox potentials are a consequence of the number of methylenic units bonding the amines and the effective overlap involved in the Cu—N bonding that is a influenced by the ligand geometry.

DNA−Copper Complex Interaction Studies. The mode and propensity of binding of the Cu(I) complexes to DNA were studied by CD spectroscopy to observe changes in the DNA secondary structure, EM in agarose gel to appreciate changes in the DNA tertiary structure, and

(18) Fabrizzi, L.; Pallavinici, P.; Parodi, L.; Perotti, A.; Taglietti, A. *J. Chem. Soc., Chem. Commun.* **1995**, *23*, 2439–2440.

(19) (a) Haiyan, Ma.; Allmendiger, M.; Thewalt, U.; Lentz, A.; Klinga, M.; Rieger, B. *Eur. J. Inorg. Chem.* **2002**, 2857–2867. (b) Koval, I. A.; Belle, C.; Selmeczi, K.; Philouze, C.; Saint-Aman, E.; Schuitema, A. M.; Gamez, P.; Pierre, J. L.; Reedijk, J. *J. Biol. Inorg. Chem.* **2005**, *10*, 739–750. (c) Mizuno, M.; Hayashi, H.; Fujinami, S.; Furutachi, H.; Nagatomo, S.; Otake, S.; Uozumi, K.; Suzuki, M.; Kitagawa, T. *Inorg. Chem.* **2003**, *42*, 8534–8544.

(20) Costas, M.; Ribas, X.; Poater, A.; López Balvuena, J. M.; Xifra, R.; Company, A.; Duran, M.; Solà, M.; Llobet, A.; Corbella, M.; Usón, M. A.; Mahía, J.; Solans, X.; Shan, X.; Benet-Buchholz, J. *Inorg. Chem.* **2006**, *45*(9), 3569–3581.

(21) Costas, M; Xifra, R; Llobet, A; Solà, M; Robles, J; Parella, T; Stoeckli-Evans, H; Neuburger, M. *Inorg. Chem.* **2003**, *42*(14), 4456–4468.

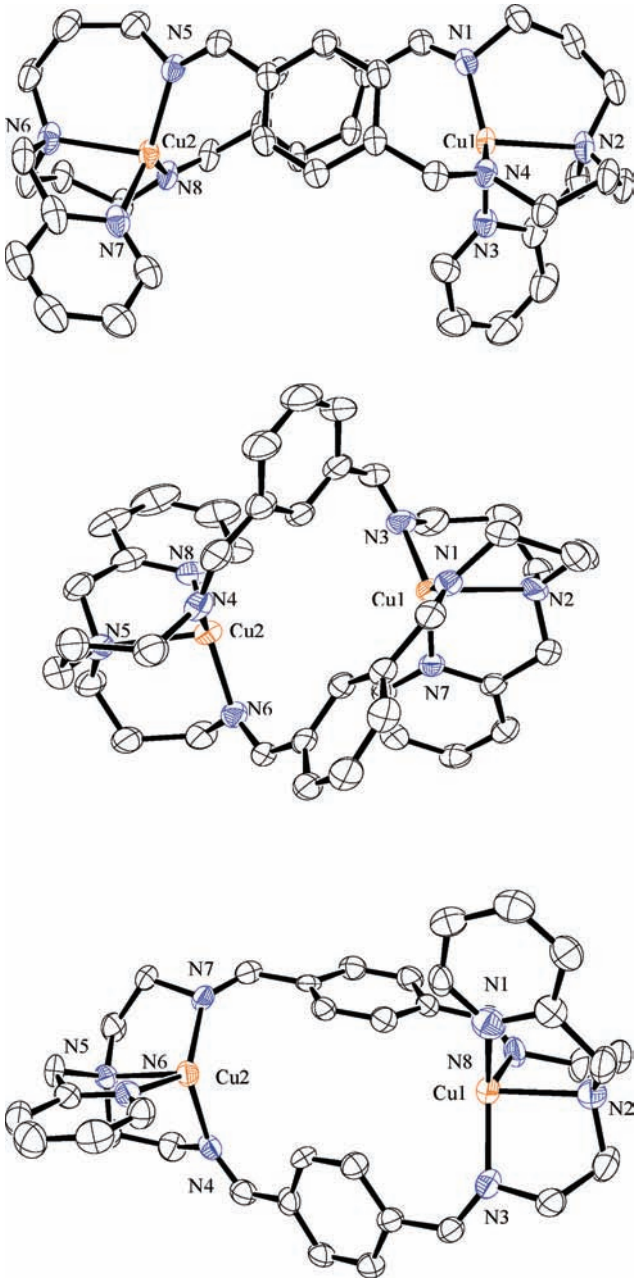

Figure 1. ORTEP plots (80% probability) for the cationic structures of the Cu(I) complexes: $\mathbf{1}^{2+}$ (top), $\mathbf{2}^{2+}$, (middle) and $\mathbf{3}^{2+}$ (bottom).

AFM to visualize changes in the DNA topography and morphology.

CD Spectroscopy. The CD spectra of CT DNA incubated 24 h at 37 °C with the corresponding copper complexes at several ratios (r_i = 0.1, 0.3, 0.5) were recorded (see Figure S18, Supporting Information). The DMSO used for the sample preparation presents some overlapping bands near the minima of ellipticity but does not interfere at the corresponding maxima.[22] For complexes **1**−**3** no large perturbations in ellipticity and wavelength of the two bands on the CD spectra of CT DNA are observed, although some slight differences can be appreciated. This indicates that the stacking mode and the orientation of base pairs in DNA is slightly disturbed, and thus the B-form character of CT DNA is still maintained. Therefore, the nature of the interaction of the Cu(I) complexes with DNA is mainly of a nonintercalative type.[10,23] This can also be supported by the crystal structures of the different Cu(I) complexes described in this work, since their geometrical nature does not produce a good fit for DNA with this type of interaction. These conclusions are in agreement with previously reported examples in the literature that have shown that the right-handed B form of free CT DNA shows a typical CD spectrum with a positive band (maximum about 268−272 nm) due to base stacking and a negative band (maximum about 245−243 nm) due to right-handed helicity[24−26] and that the intercalation of small molecules to DNA would cause a characteristic decrease in both positive and negative bands.[10] On the other hand simple groove binding and electrostatic interaction of small molecules with DNA shows little or no perturbations on the two bands[24,27] as observed in our case.

EM. The influence of complexes **1**−**3** on the tertiary structure of DNA was determined by its ability to modify the EM of the pBR322 plasmid DNA, which presents a circular shape with two main forms: a relaxed open circular form (OC) and a supercoiled covalently closed form (CCC) that is much more compacted than the former one. The EM of these two forms is very different since the EM is also a function of the degree of folding.

In Figure 2 it is presented the EM of complexes **1**−**3** (r_i = 6.9) in the absence and presence of H_2O_2, showing their capacity to promote important changes in the EM of the pBR322 plasmid DNA under aerobic and physiological conditions (pH 7.0, 37 °C). Time course experiments reveal that, without H_2O_2, all complexes are capable of inducing conversion of supercoiled plasmid DNA form (CCC) into relaxed circular form (OC) (lanes 1, 4, and 7 for complexes **1**, **2**, and **3** respectively) and other slower moving forms of DNA (bands migrating higher than OC) (lanes 1 and 4 for complexes **1** and **2**, respectively). The degree of induction under these conditions is **1** > **2** ≫ **3**, as is evident from the relative decrease in the intensity of the supercoiled bands.

The addition of H_2O_2, with different exposition times, produces much stronger damage to the DNA than the Cu(I) alone for cases **1** and **2** (see lanes, 2−3 for complex **1** and 5−6 for **2**) but now the relative reactivity is reversed; that is, **2** is more active than **1**. In sharp contrast the addition of H_2O_2 to complex **3** (lanes 8−9) basically does not modify its activity as compared to its performance without H_2O_2. Under similar conditions no cleavage of pBR322 DNA occurred for free H_2O_2 (see Supporting Information).

(22) (a) Moradell, S.; Lorenzo, J.; Rovira, A.; Robillard, M. S.; Avilés, F. X.; Moreno, V.; de Llorens, R.; Martinez, M. A.; Reedijk, J.; Llobet, A. *J. Inorg. Biochem.* **2003**, *96*/*4*, 493–502. (b) Moradell, S.; Lorenzo, J.; Rovira, A.; van Zutphen, S.; Avilés, F. X.; Moreno, V.; Llorens, R.; Martinez, M. A.; Reedijk, J.; Llobet, A. *J. Inorg. Biochem* **2004**, *98*, 1933–1946.

(23) (a) McMillin, D. R.; McNett, K. M. *Chem. Rev.* **1998**, *98*, 1201–1220. (b) Mounir, M.; Lorenzo, J.; Ferrer, M.; Prieto, M. J.; Rosell, O.; Avilès, F. X.; Moreno, V. *J. Inorg. Biochem.* **2007**, *101*, 660–666.

(24) Kong, D.-M.; Wang, J.; Zhu, L.-N.; Jin, Y.-W.; Li, X.-Z.; Shen, H.-X.; mi, H.-F. *J. Inorg. Biochem.* **2008**, *102*, 824–832.

(25) Rajendran, A.; Nair, B. U. *Biochim. Biophys. Acta* **2006**, *1760*, 179–1801.

(26) Lincoln, P.; Tuite, E.; Norden, B. *J. Am. Chem. Soc.* **1997**, *119*, 1454.

(27) Li, J.-H.; Wang, J.-T.; Hu, P.; Zhang, L.-Y.; Chen, Z.-N.; Mao, Z.-W.; Ji, L.-N. *Polyhedron* **2008**, *27*, 1898–1904.

Table 2. Selected Bond Lengths (Å) and Angles (deg) for **1**$(CF_3SO_3)_2$, **2**$(SbF_6)_2$, and **3**$(CF_3SO_3)_2$

$[Cu_2^I(bsp3py)](CF_3SO_3)_2$ (**1**$(CF_3SO_3)_2$)		$[Cu_2^I(bsm3py)](SbF_6)_2$ (**2**$(SbF_6)_2$)		$[Cu_2^I(bsp2py)](CF_3SO_3)_2$ (**3**$(CF_3SO_3)_2$)	
$Cu(1)—N_{im}(1)$	1.959(4)	$Cu(1)—N_{im}(1)$	1.985(3)	$Cu(1)—N_{im}(3)$	1.983(3)
$Cu(1)—N_{im}(4)$	1.993(4)	$Cu(1)—N_{im}(3)$	1.987(3)	$Cu(1)—N_{im}(8)$	2.032(3)
$Cu(1)—N_{py}(3)$	2.073(4)	$Cu(1)—N_{py}(7)$	2.031(3)	$Cu(1)—N_{py}(1)$	2.004(3)
$Cu(1)—N_{ter}(2)$	2.205(4)	$Cu(1)—N_{ter}(2)$	2.206(3)	$Cu(1)—N_{ter}(2)$	2.207(3)
$Cu(2)—N_{im}(8)$	2.002(4)	$Cu(2)—N_{im}(6)$	1.982(3)	$Cu(2)—N_{im}(7)$	1.985(3)
$Cu(2)—N_{im}(5)$	2.002(4)	$Cu(2)—N_{im}(4)$	2.005(3)	$Cu(2)—N_{im}(4)$	2.018(3)
$Cu(2)—N_{py}(7)$	2.031(4)	$Cu(2)—N_{py}(8)$	2.019(3)	$Cu(2)—N_{py}(6)$	2.038(3)
$Cu(2)—N_{ter}(6)$	2.221(4)	$Cu(2)—N_{ter}(5)$	2.203(3)	$Cu(2)—N_{ter}(5)$	2.200(3)
Cu(1)—Cu(2)	7.364	Cu(1)—Cu(2)	4.517	Cu(1)—Cu(2)	6.956
$N_{im}(1)—Cu(1)—N_{im}(4)$	131.71(15)	$N_{im}(1)—Cu(1)—N_{im}(3)$	121.37(14)	$N_{im}(3)—Cu(1)—N_{im}(8)$	116.30(12)
$N_{im}(1)—Cu(1)—N_{py}(3)$	125.60(16)	$N_{im}(1)—Cu(1)—N_{py}(7)$	123.62(13)	$N_{im}(3)—Cu(1)—N_{py}(1)$	129.81(12)
$N_{im}(4)—Cu(1)—N_{py}(3)$	100.33(15)	$N_{im}(3)—Cu(1)—N_{py}(7)$	114.87(13)	$N_{im}(8)—Cu(1)—N_{py}(1)$	110.72(11)
$N_{im}(1)—Cu(1)—N_{ter}(2)$	99.70(16)	$N_{im}(1)—Cu(1)—N_{ter}(2)$	95.51(13)	$N_{im}(3)—Cu(1)—N_{ter}(2)$	85.90(11)
$N_{im}(4)—Cu(1)—N_{ter}(2)$	102.32(15)	$N_{im}(3)—Cu(1)—N_{ter}(2)$	97.05(13)	$N_{im}(8)—Cu(1)—N_{ter}(2)$	85.25(11)
$N_{py}(3)—Cu(1)—N_{ter}(2)$	80.12(15)	$N_{py}(7)—Cu(1)—N_{ter}(2)$	81.02(12)	$N_{py}(1)—Cu(1)—N_{ter}(2)$	81.32(11)
$N_{im}(8)—Cu(2)—N_{im}(5)$	113.13(17)	$N_{im}(6)—Cu(2)—N_{im}(4)$	119.84(13)	$N_{im}(7)—Cu(2)—N_{im}(4)$	125.76(12)
$N_{im}(8)—Cu(2)—N_{py}(7)$	119.68(16)	$N_{im}(6)—Cu(2)—N_{py}(8)$	122.54(13)	$N_{im}(7)—Cu(2)—N_{py}(6)$	120.05(12)
$N_{im}(5)—Cu(2)—N_{py}(7)$	126.64(16)	$N_{im}(4)—Cu(2)—N_{py}(8)$	117.60(13)	$N_{im}(4)—Cu(2)—N_{py}(6)$	111.21(12)
$N_{im}(8)—Cu(2)—N_{ter}(6)$	98.11(15)	$N_{im}(6)—Cu(2)—N_{ter}(5)$	95.29(13)	$N_{im}(7)—Cu(2)—N_{ter}(5)$	85.46(11)
$N_{im}(5)—Cu(2)—N_{ter}(6)$	97.97(15)	$N_{im}(4)—Cu(2)—N_{ter}(5)$	94.89(13)	$N_{im}(4)—Cu(2)—N_{ter}(5)$	85.41(11)
$N_{py}(7)—Cu(2)—N_{ter}(6)$	82.21(17)	$N_{py}(8)—Cu(2)—N_{ter}(5)$	81.14(13)	$N_{py}(6)—Cu(2)—N_{ter}(5)$	81.70(12)

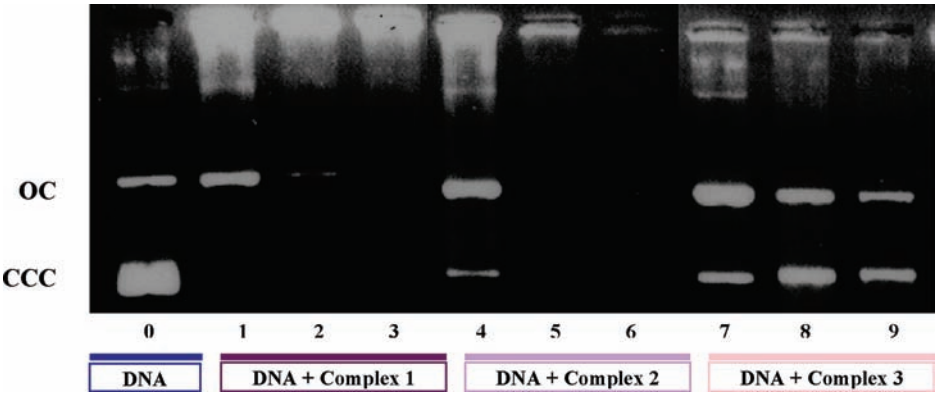

Figure 2. Agarose gel EM of pBR322 plasmid DNA treated with Cu(I) compounds (DNA concentration 0.017 μg/μL, 6×10^{-3} μM, molar ratio $r_i = 6.9$; r_i: input molar ratio of the complex to nucleotide). Incubation time 2 h (37 °C). Lane 0, pBR322 plasmid DNA; Lane 1, DNA + Complex **1**; Lane 2, DNA + complex **1** treated with 1 μL H_2O_2 (33% w/v) for $t = 3$ min, after incubation; Lane 3, DNA + complex **1** treated with 1 μL H_2O_2 (33% w/v) for $t = 30$ min, after incubation; Lane 4, DNA + complex **2**; Lane 5, DNA + complex **2** treated with 1 μL H_2O_2 (33% w/v) for $t = 3$ min, after incubation; Lane 6, DNA + complex **2** treated with 1 μL H_2O_2 (33% w/v) for $t = 30$ min, after incubation; Lane 7, DNA + complex **3**; Lane 8, DNA + complex **3** treated with 1 μL H_2O_2 (33% w/v) for $t = 3$ min, after incubation; Lane 9, DNA + complex **3** treated with 1 μL H_2O_2 (33% w/v) for $t = 30$ min, after incubation. (OC, open circular form; CCC, covalently closed circular form).

Electrophoresis of complexes **1**−**3** ($r_i = 6.9$), under anaerobic conditions, in the absence of H_2O_2, has also been performed (Figure S20, Supporting Information). The results show that all complexes can effectively promote similar changes in the EM of the pBR322 plasmid DNA to those obtained under aerobic conditions suggesting that atmospheric oxygen is not involved in the cleavage process. The results obtained are consistent with the fact that copper(I) complexes examined here are capable of promoting important interactions with DNA, producing a sequential decrease of the CCC form folding, but do not cleave pBR322 plasmid DNA in the absence of hydrogen peroxide. We think that these interactions lead to relaxed open conformation (bands OC) and other aggregation of DNA molecules originated by cross-links between the complexes and more or less relaxed different molecules of plasmid DNA (bands migrating higher than OC) in agreement with the results observed in EF (Figure 2). The nuclease activity of these copper(I) complexes take place by direct strand scission when H_2O_2 is present. The DNA degraded completely into small pieces, and it could not induce the linear form in the tested experiment.

AFM. Direct visualization of three conformers of plasmid DNA can be achieved using tapping mode atomic force microscopy (TMAFM) and thus allows graphically evaluating plasmid DNA cleavage by metallonucleases.[2,28]AFM images of free pBR322 plasmid DNA and pBR322 incubated with complexes **1**−**3** ($r_i = 6.9$) with and without H_2O_2 under the same conditions as in the EM experiments are presented in Figures 3 and S21, Supporting Information.

Image b in Figure 3 shows the plasmid DNA modifications produced by **1**, where the largest part of DNA has started to relax in the OC form DNA, although it is

(28) (a) Coury, J. E.; McFail-Isom, L.; Williams, L. D.; Bottomley, L. A. *Proc. Natl. Acad. Sci. U.S.A.* **1996**, *93*, 12283. (b) Coury, J. E.; Anderson, J. R.; McFail-Isom, L.; Williams, L. D.; Bottomley, L. A. *J. Am. Chem. Soc.* **1997**, *119*, 3792.

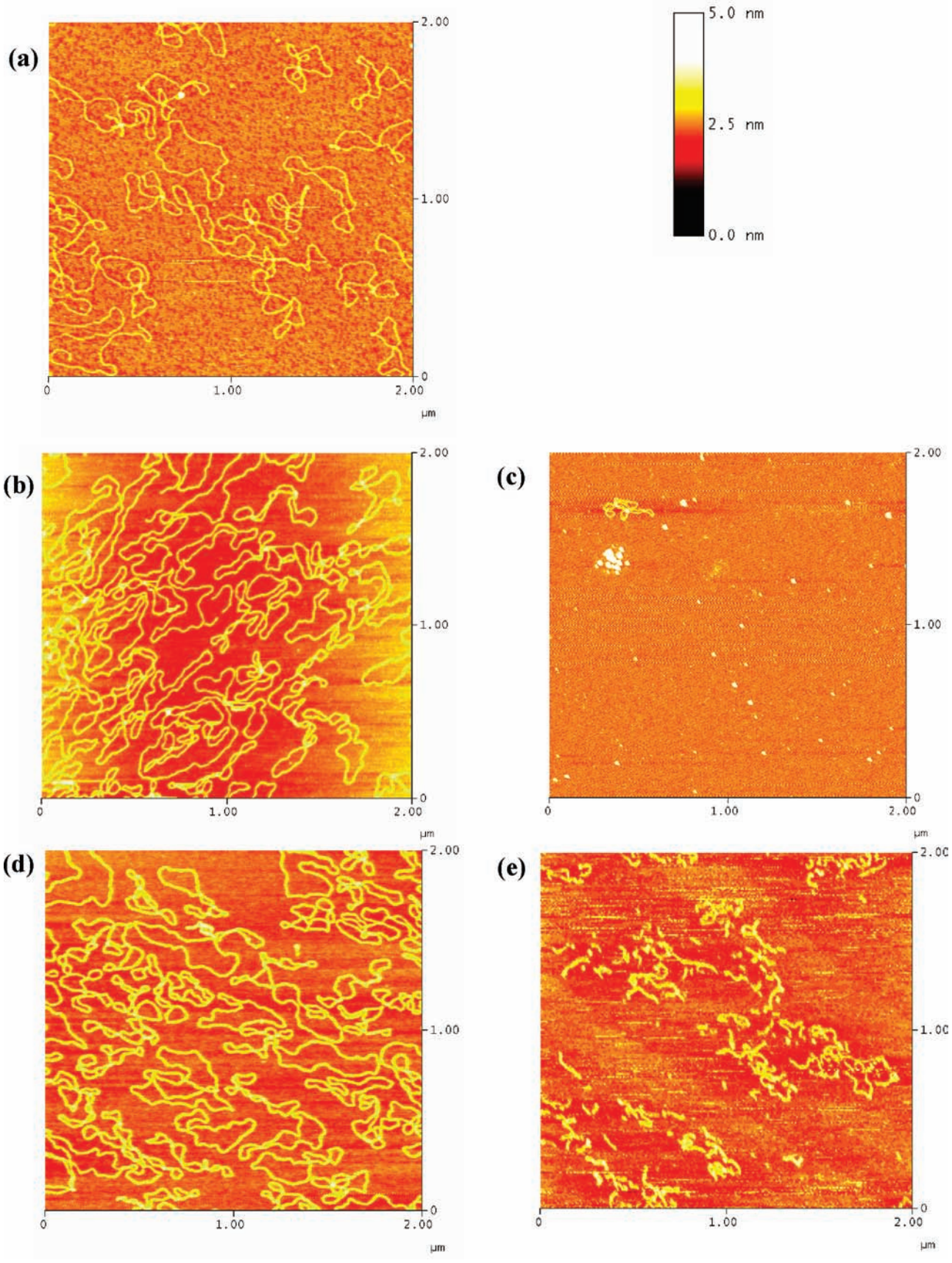

Figure 3. TMAFM images of pBR322 plasmid DNA treated with Cu(I) compounds (DNA concentration 0.0043 μg/μL, 1.5×10^{-3} μM, molar ratio r_i = 6.9; r_i: input molar ratio of the complex to nucleotide) (a) free pBR322 DNA; (b) pBR322 DNA incubated with **1**, 2 h (37 °C); (c) pBR322 DNA incubated with **1**, 2 h (37 °C), sample treated with 1 μL H_2O_2 (33% w/v) for t = 30 min, after incubation; (d) pBR322 DNA incubated with **2**, 2 h (37 °C); (e) pBR322 DNA incubated with **2**, 2 h (37 °C), sample treated with 1 μL H_2O_2 (33% w/v) for t = 2 min, after incubation.

possible to observe some molecules with an intermediate degree of folding and some others containing several crossing points. Image c, taken 2 min after the addition of 1 μL of H_2O_2, shows that most of the DNA has been completely destroyed as a result of the cleavage activity of the complex. Image d in Figure 3 shows the effect produced by **2** where CCC and OC DNA forms can be observed. The addition of H_2O_2 is shown in image e where, after 3 min, complex **2** exhibits clear evidence of DNA-strand scission to give short fragments.

Finally, Figure S21a (Supporting Information) shows the reaction of **3** with the plasmid DNA where CCC and OC forms can be observed. Images b and c show the effect of adding H_2O_2 together with complex **3**, showing that it is able to cause a small amount of double strand scission of pBR322 but not able to fully convert the CCC form into the OC form. This behavior is in agreement with the results observed in the EM pattern.

Discussion

Complexes **1**−**3** belong to a family of dinuclear Cu(I) complexes containing octaaza dinucleating macrocyclic ligands that can be envisaged as formed by a phenylic spacer linked to two different coordination sites (see Chart 1). The properties of these ligands are finely modulated by changing the number of methylenic spacers between the aminic N atoms and by the meta or para substitution at the aromatic spacer. These small variations in the ligands produce a significantly different 3D topography for the three Cu(I) complexes **1**−**3**, as revealed by their crystal structures (see Figure 1) described in the previous section. On the other hand the redox properties of the metal centers change depending on the macrocyclic ligand used as indicated in the previous section.

CD spectroscopy indicates that the interaction of complexes **1**−**3** with DNA is weak, not of an intercalative nature, and thus due mainly to electrostatic and H-bonding type of interactions. Under EM conditions with no peroxide, the supramolecular complex generated is then responsible for the transformation of the CCC form of the DNA into the OC. The different reactivities of the complexes **1**−**3** are thus associated with the two differentiated properties of the complexes: the redox potential and the shape of the molecule. With regard to the latter it is interesting to bear in mind the work of Rodger et al. and others[29,30] for dinuclear Fe(II) complexes where relative orientation of the aromatic rings play a key role in the non-intercalating interaction with DNA. In our particular case it is important to realize that for the para-substituted cases **1** and **3**, the relative orientation of their pyridylic rings will dictate the degree of interaction with DNA. Thus a quasi-orthogonal disposition of this type of nonintercalative supramolecular interaction will generate a very weak interaction (which is the case for complex **3**) whereas a 50.88° angle will produce a chelate sort of interaction with the two pyridylic rings properly oriented and thus be able to produce a much stronger interaction (which is the case of complex **1**).[29] For the meta case, complex **2**, its spherical shape also seems to have a good contact with DNA as evidenced by having a relative similar interaction as with **1** under similar redox potentials conditions.

We have recently shown that the reaction of related Cu(I) complexes, containing similar macrocyclic ligands with no pyridylic pendant arms, with oxygen generates Cu_2O_2 peroxo type of intermediates.[20,31] In the case of the complexes where the macrocyclic ligand has a para substitution, a *trans*-μ-1,2-peroxo is formed due to the large distance between the Cu centers imposed by spacer. However, in the case of the meta the distance is highly reduced and a $\mu-\eta_2:\eta_2$-peroxo is formed. The different nature of the peroxo complex formed can be responsible for the reversal of reactivity observed for the Cu(I) complexes in the presence of H_2O_2. On the other hand the much lesser activity of complex **3** is hampered by the weak supramolecular interaction of the plain Cu(I) complex that seems to be a requirement for the reaction with DNA to proceed.

Finally the relatively similar reactivity observed for complex **3** in the presence and absence of hydrogen peroxide and the different reactivity of **1** and **2** with H_2O_2 rule out the formation of free hydroxyl radical species and point out that the main chemistry produced in our case is nucleophilic addition of peroxide to the Cu(I) complex, in a similar manner as had been found in previous reports with related complexes.[32]

As a conclusion, the present work shows how small variations in the ligand backbone can cause significant differences in their respective Cu(I) complexes that in turn are responsible for radically differentiated biological reactivity.

Acknowledgment. This research has been financed by MICINN of Spain through projects BQU 2005-01834, CTQ2007-67918, and CSD2006-0003. A.A. is grateful for the award of a doctoral grant from CIRIT Generalitat de Catalunya. X.S. also thanks MICINN for a Torres Quevedo Contract.

Supporting Information Available: Crystallographic information files (CIF) for **1**$(CF_3SO_3)_2$, **2**$(SbF_6)_2$, and **3**$(CF_3SO_3)_2$, additional spectroscopic data for the organic compounds and copper complexes, FT-IR studies for CO adducts, electrochemical characterization, DC spectra, additional EF controls, and AFM images. This material is available free of charge via the Internet at http://pubs.acs.org.

(29) Khalid, S.; Hannon, M. J.; Rodger, A.; Rodger, P. M. *Chem.—Eur. J.* **2006**, *12*, 3493–3506.
(30) Boer, D. Roeland; Canals, A.; Coll, M. *Dalton Trans.* **2009**, 399–414.
(31) Poater, A.; Ribas, X.; Llobet, A.; Cavallo, L.; Solà, M. *J. Am. Chem. Soc.* **2008**, *130*(52), 17710–17717.
(32) (a) Sawyer, D. T.; Kang, C.; Llobet, A. *J. Am. Chem. Soc.* **1993**, *115* (13), 5817–5818. (b) Sobkowiak, A.; Qui, A.; Liu, X.; Llobet, A.; Sawyer, D. T. *J. Am. Chem. Soc.* **1993**, *115*(2), 609–614.